

Baryonic Regge trajectories with analyticity constraints

R. Fiore^{a†}, L. L. Jenkovszky^{b‡}, F. Paccanoni^{c*}, A. Prokudin^{d◇}

^a *Dipartimento di Fisica, Università della Calabria and
Istituto Nazionale di Fisica Nucleare, Gruppo collegato di Cosenza
I-87036 Arcavata di Rende, Cosenza, Italy*

^b *Bogolyubov Institute for Theoretical Physics
Academy of Science of Ukraine
UA-03143 Kiev, Ukraine*

^c *Dipartimento di Fisica, Università di Padova and
Istituto Nazionale di Fisica Nucleare, Sezione di Padova
Via F. Marzolo 8, I-35131 Padova, Italy*

^d *Dipartimento di Fisica Teorica, Università di Torino,
Istituto Nazionale di Fisica Nucleare, Sezione di Torino
Via P. Giuria 1, I-10125 Torino, Italy and
Institute for High Energy Physics, 142284 Protvino, Russia*

A model for baryonic Regge trajectories compatible with the threshold behavior required by unitarity and asymptotic behavior in agreement with analyticity constraints is given in explicit form. Widths and masses of the baryonic resonances on the N and Δ trajectories are reproduced. The MacDowell symmetry is exploited and an application is given.

[†]*e-mail address:* FIORE@CS.INFN.IT

[‡]*e-mail address:* JENK@GLUK.ORG

^{*}*e-mail address:* PACCANONI@PD.INFN.IT

[◇]*e-mail address:* PROKUDIN@TO.INFN.IT

1 Introduction

The dynamical origin of the meson mass spectra and the analytic properties of the bosonic Regge trajectories have been studied thoroughly in the past and a comprehensive review on this subject can be found in Ref. [1]. The same statement does not hold for baryons that present further complications due to their more involved internal structure and, as we shall see, to the intricate analytical properties of their Regge trajectories.

Information on the N and Δ baryon trajectories has been obtained from the analysis of backward pion-nucleon scattering, see for example, Refs. [2, 3, 4, 5], where the important problem of the linearity of the baryon Regge trajectories has been investigated in detail. The conclusion that Regge trajectories are not straight and parallel lines is supported by the detailed analysis of Ref. [6]. Moreover, in the case of baryons, the analyticity properties of the trajectory function [8], that follow from the invariance under Schwinger's space-time reflection of the covariant scattering amplitude [9], confirm this conclusion.

Since the position of the singularity in the J plane of the partial wave amplitude is an analytic function of the center of mass energy in the relevant channel, say \sqrt{s} , the MacDowell symmetry [9] implies that

$$\alpha^+(\sqrt{s}) = \alpha^-(-\sqrt{s}) \quad \text{for } s > 0, \quad (1)$$

where \pm denote the parity of the trajectory. The relation (1) requires that, if the trajectory is linear in s , parity doublets must exist. The simplest way of eliminating doublets, that are not observed experimentally, is to take into account deviations of the trajectories from linearity and to show, as in Ref. [5], that these deviations are compatible with experimental data. Arguments based on the spontaneous chiral symmetry breaking in the low energy part of the baryon spectrum [10] support this point of view.

For the above reasons, attempts to exploit the explicit form of the baryon trajectories on the basis of the experimental data only meet great difficulties. While in Ref. [4] the conclusion is that N_α and N_β are independent Regge trajectories, since otherwise it would be impossible to explain the energy dependence of $\pi^+ p$ backward cone and the dip, the parametrization of Ref. [5] succeeds in reproducing the baryon spectrum, the energy dependence of cross sections and the momentum transfer dependence of differential cross sections. Dispersion relations for the trajectory function [4, 8, 11] impose severe constraints on the analytic structure of this function [12, 13] and give the opportunity to restrict its possible form.

In this paper we construct an explicit model for complex Regge trajectories reproducing both the masses and widths of observed baryonic resonances with the constraints of analyticity and unitarity. Section 2 presents an attempt to adapt a previous model for meson trajectories [14, 15] to the baryon spectrum. The N and Δ trajectories are considered in detail in Section 3. In Section 4 we implement the MacDowell symmetry and derive explicit formulas for the real and imaginary parts of the trajectory. The application to the nucleon trajectory is studied in Section 5. The last Section is devoted to concluding remarks.

2 A simple model

The properties of the bosonic trajectories following from analyticity and unitarity [16] have been summarized in our previous papers [14, 15]. Fermion trajectories suffer further complications [11]. The generalization of the MacDowell symmetry shows that, in order to satisfy the relation between natural and unnatural parity amplitudes, we need two trajectories of opposite parity that are related by the relation (1). Moreover the dispersion relation for the trajectory function should exhibit analyticity in \sqrt{s} and should be written in terms of this variable. In order to clarify the problem, however, we will limit ourselves, in this Section, to consider analyticity in the variable s for a simplified model.

Let P be the parity of the resonances lying on a Regge trajectory. Since $P = \eta(-1)^{J-v}$, where $v = 1/2$ for odd half-integral J and $v = 0$ for integral J , natural parity means $\eta = +1$ while unnatural parity means $\eta = -1$. Hence for the N trajectory, $(\frac{1}{2}^+, \frac{5}{2}^+, \dots)$, we have $\eta = +1$ while, for the Δ trajectory, $(\frac{3}{2}^+, \frac{7}{2}^+, \dots)$, $\eta = -1$. The minimum allowed angular momentum is [16]

$$L = J - (s_1 + s_2) + \frac{1}{2} [1 - \eta\eta_1\eta_2 (-1)^{s_1+s_2-v}]$$

and, since $\eta_1 = -1$ for the pion and $\eta_2 = +1$ for the nucleon, the Δ trajectory function will be characterized by $L = J - \frac{1}{2}$. Both the real and imaginary part of the trajectory will inherit the threshold behavior of the partial wave amplitude for pion-nucleon scattering:

$$(q_{12}^2)^{L+1/2} = (q_{12}^2)^J, \quad (2)$$

where q_{12} is the center of mass momentum.

While retaining the assumption of additivity of threshold contributions, the more regular behavior of the baryonic resonance widths suggest that the choice of the imaginary part of the trajectory can be different from the bosonic case. As a first attempt, we consider analyticity in s for the trajectory functions and start from the simple form for the imaginary part of the trajectory

$$\mathcal{I}m\alpha(s) = s^\delta \sum_n c_n \left(\frac{s - s_n}{s} \right)^{\mathcal{R}e\alpha(s_n)} \cdot \theta(s - s_n). \quad (3)$$

Eq. (3) has the correct threshold behaviour and analyticity requires that $\delta < 1$. The boundedness of $\alpha(s)$ for $s \rightarrow \infty$ follows from the condition that the amplitude, in the Regge form, should have no essential singularity at infinity in the cut plane.

The once subtracted dispersion relation for the trajectory is

$$\mathcal{R}e\alpha(s) = \alpha(0) + \frac{s}{\pi} PV \int_0^\infty ds' \frac{\mathcal{I}m\alpha(s')}{s'(s' - s)}, \quad (4)$$

where PV means the Cauchy principal value of the integral. Setting $\lambda_n = \mathcal{R}e\alpha(s_n)$ we get

$$\mathcal{R}e\alpha(s) = \alpha(0) + \frac{s}{\pi} \sum_n c_n \mathcal{A}_n(s), \quad (5)$$

where [18]

$$\begin{aligned} \mathcal{A}_n(s) = & \frac{\Gamma(1-\delta)\Gamma(\lambda_n+1)}{\Gamma(\lambda_n-\delta+2)s_n^{1-\delta}} {}_2F_1\left(1, 1-\delta; \lambda_n-\delta+2; \frac{s}{s_n}\right) \theta(s_n-s) + \\ & \left\{ \pi s^{\delta-1} \left(\frac{s-s_n}{s}\right)^{\lambda_n} \cot[\pi(1-\delta)] - \right. \\ & \left. \frac{\Gamma(-\delta)\Gamma(\lambda_n+1)s_n^\delta}{s\Gamma(\lambda_n-\delta+1)} {}_2F_1\left(\delta-\lambda_n, 1; \delta+1; \frac{s_n}{s}\right) \right\} \theta(s-s_n). \end{aligned}$$

From these equations we get the slope

$$\mathcal{R}e \alpha'(s) = \frac{1}{\pi} \sum_n c_n \mathcal{B}_n(s), \quad (6)$$

where

$$\begin{aligned} \mathcal{B}_n(s) = & \frac{\Gamma(1-\delta)\Gamma(\lambda_n+1)}{\Gamma(\lambda_n-\delta+2)s_n^{1-\delta}} {}_2F_1\left(2, 1-\delta; \lambda_n-\delta+2; \frac{s}{s_n}\right) \theta(s_n-s) + \\ & \left\{ \pi s^{\delta-1} \left(\frac{s-s_n}{s}\right)^{\lambda_n} \cot[\pi(1-\delta)] \left(\delta + \lambda_n \frac{s_n}{s-s_n}\right) - \right. \\ & \left. \frac{\Gamma(-\delta)\Gamma(\lambda_n+1)s_n^{\delta+1}}{(1+d)\Gamma(\lambda_n-\delta)s^2} {}_2F_1\left(1+\delta-\lambda_n, 2; \delta+2; \frac{s_n}{s}\right) \right\} \theta(s-s_n). \end{aligned}$$

Eqs. (3) and (6) determine the widths of the resonances through the relation

$$\Gamma = \frac{\mathcal{I}m \alpha(M^2)}{M \mathcal{R}e \alpha'(M^2)}, \quad (7)$$

where Γ is the total width of the resonance and M is its mass.

3 Fitting the resonances masses and widths in the simplified model

In this section we apply the formalism to the Δ baryon trajectory ($\frac{3}{2}^+, \frac{7}{2}^+, \dots$) and nucleon N^+ trajectory which contains baryons $N(939) \frac{1}{2}^+$, $N(1680) \frac{5}{2}^+$, $N(2220) \frac{9}{2}^+$ and $N(2700) \frac{13}{2}^+$ [7]. In the fit the input data are the masses and widths of the resonances. The quantities to be determined are the parameters c_n , δ and the thresholds s_n . While s_1 is fixed to the pion-nucleon threshold, data allow for the determination of other two thresholds at maximum. i.e. s_2 and a higher threshold, the one above all the known resonances, that will be called s_x in the following.

3.1 Δ^+ trajectory

First we fit the real part of the amplitude using a linear form of the trajectory

$$\mathcal{R}e\alpha(s) = \alpha(0) + \alpha'(0) \cdot s . \quad (8)$$

Thus we obtain $\alpha(0) = 0.17 \pm 0.02$ and $\alpha'(0) = 0.87 \pm 0.01$ (GeV^{-2}) ($\chi^2/\text{d.o.f} = 0.63$). Using these values of the parameters we calculate $\mathcal{R}e\alpha(s_n)$, where $n = 1, 2, x$ and $s_1 = (m_\pi + m_N)^2 = 1.16 \text{ GeV}^2$, $s_2 = 2.8 \text{ GeV}^2$ and $s_x = 15 \text{ GeV}^2$.

Then, as previously stated, we set $\lambda_n = \mathcal{R}e\alpha(s_n)$ and continue the recursive fitting procedure using formulas (5) and (6). After 15 steps the procedure converges and we obtain the values of the parameters: $\alpha(0) = -0.04 \pm 0.03$, $\delta = -0.26 \pm 0.01$, $c_1 = 0.75 \pm 0.03$, $c_2 = 2.2 \pm 0.3$ and $c_x = 1414 \pm 75$, $s_2 = 2.44 \pm 0.05 \text{ GeV}^2$, $s_x = 11.7 \pm 0.3 \text{ GeV}^2$ ($\chi^2/\text{d.o.f} = 1.4$).

Δ resonances have been seen in a large number of formation and production experiments. $\Delta(1950)$ has been seen in the ΣK channel, $\pi^+ p \rightarrow \Sigma^+ K^+$, but the evidence is poor, and one of its decay modes is $N\rho$, ($< 10\%$). It is interesting to notice that the threshold in the ΣK channel, for example, is 2.84 GeV^2 and for $N\rho$ is 2.92 GeV^2 . Both are higher than, but not too far from, the second threshold $s_2 = 2.44 \text{ GeV}^2$ found empirically minimizing the χ^2 of the fit.

The results are shown in figures 1 and 2.

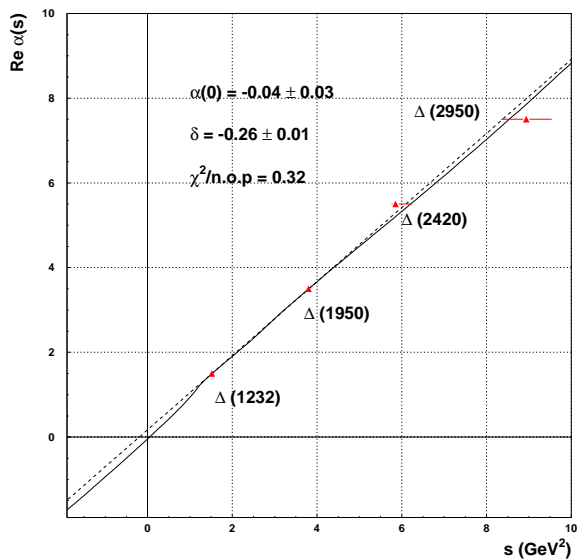


Figure 1: The real part of Δ trajectory. The dashed line corresponds to the result of a linear fit, the solid line corresponds to the final result.

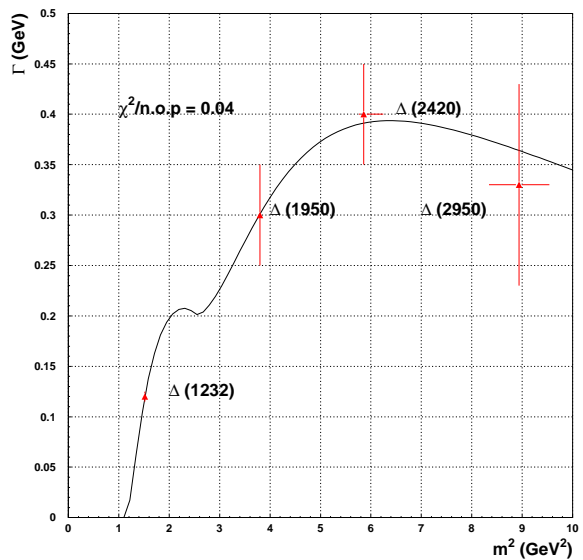


Figure 2: The width of Δ trajectory.

3.2 N^+ trajectory

As in the previous Subsection, we start fitting the real part of the amplitude using a linear form of the trajectory:

$$\mathcal{R}e\alpha(s) = \alpha(0) + \alpha'(0) \cdot s . \quad (9)$$

Thus we obtain $\alpha(0) = -0.27 \pm 0.14$ and $\alpha'(0) = 0.98 \pm 0.04$ (GeV^{-2}) ($\chi^2/\text{d.o.f} = 0.24$). Using these values of the parameters we calculate $\text{Re} \alpha(s_n)$, where $n = 1, 2, x$ and $s_1 = (m_\pi + m_N)^2 = 1.16 \text{ GeV}^2$, $s_2 = 2.44 \text{ GeV}^2$ and $s_x = 11.7 \text{ GeV}^2$. Now the channels $N\eta$, with a threshold at 2.21 GeV^2 , and ΛK , with a threshold at 2.59 GeV^2 , are no more forbidden. Also in the N^+ the interpretation of the second threshold as a physical one seems now appropriate.

Then we set $\lambda_n = \text{Re} \alpha(s_n)$ and continue the recursive fitting procedure using formulas (5) and (6). Again after 15 steps the procedure converges and we obtain the values of the parameters: $\alpha(0) = -0.41$, $\delta = -0.46 \pm 0.07$, $c_1 = 0.51 \pm 0.08$, $c_2 = 4.0 \pm 0.8$ and $c_x = (4.5 \pm 1.7) \cdot 10^4$ ($\chi^2/\text{d.o.f} = 1.15$).

The results are depicted in figs. 3 and 4.

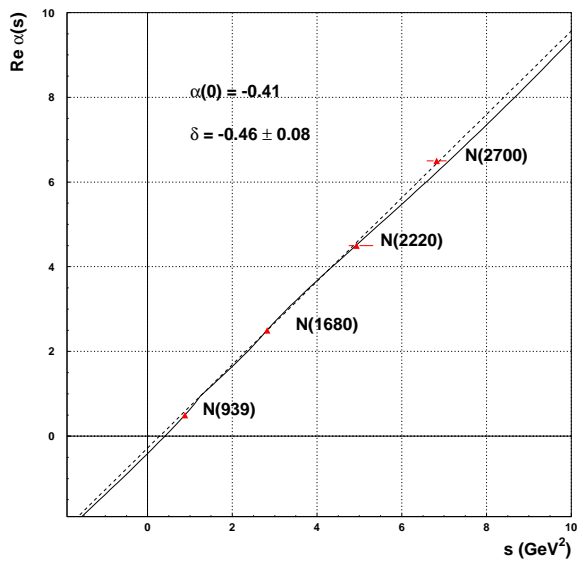


Figure 3: The real part of N trajectory. The dashed line corresponds to the result of a linear fit, the solid line corresponds to the final result.

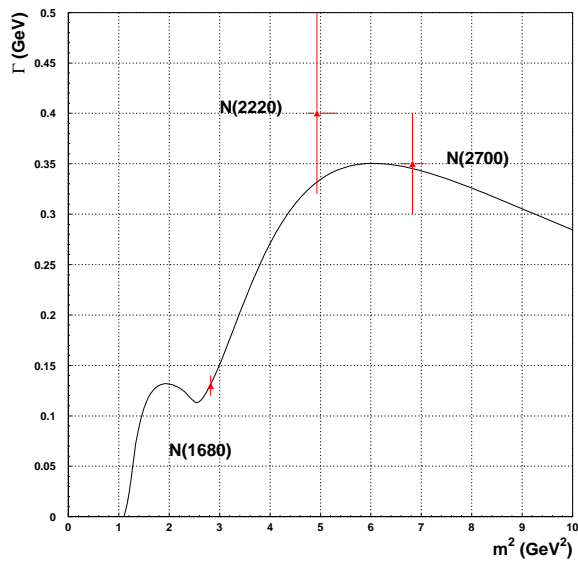


Figure 4: The width of N trajectory.

4 An approach based on MacDowell symmetry

The trajectories of baryonic Regge poles in states with angular momentum J and parity $(-1)^{J+1/2}$ coincide when the c.m. energy squared s tends to zero and become complex conjugate of each other for $s < 0$ [8]. This relation is due to the kinematic singularity \sqrt{s} present in spinor amplitudes. The trajectory function $\alpha = \alpha(\sqrt{s})$ is complex for $\sqrt{s} > \sqrt{s_1}$ and $\sqrt{s} < -\sqrt{s_1}$ and real in the interval $-\sqrt{s_1} < \sqrt{s} < \sqrt{s_1}$ where s_1 is the first threshold, $s_1 = (m_\pi + m_N)^2 = 1.16 \text{ GeV}^2$ for Δ and N trajectories. A dispersion relation can be written for $\alpha(\sqrt{s})$ [8, 2, 11]:

$$\alpha(\sqrt{s}) = \frac{1}{\pi} \int_{\sqrt{s_1}}^{\infty} \frac{\text{Im} \alpha^+(s')}{\sqrt{s'} - \sqrt{s}} d\sqrt{s'} + \frac{1}{\pi} \int_{\sqrt{s_1}}^{\infty} \frac{\text{Im} \alpha^-(s')}{\sqrt{s'} + \sqrt{s}} d\sqrt{s'}, \quad (10)$$

where $\mathcal{I}m \alpha^\pm(s)$ are the imaginary parts of the position of the poles of the $\pi - N$ scattering amplitudes in states with angular momentum α and parity $(-1)^{\alpha \pm 1/2}$.

The MacDowell symmetry for the $\pi - N$ partial waves amplitudes [9],

$$T_{J-1/2}^J(\sqrt{s}) = T_{J+1/2}^J(-\sqrt{s}) , \quad (11)$$

implies the existence of resonance states with the same J , but opposite parity, except when their residue vanishes. Hence the possibility to reveal these additional resonances, and confirm their existence, depends on the detailed behavior of the residue function [17, 2, 3]¹.

In the following we will consider the N -trajectory and express the $\ell = J + 1/2$ amplitude through the $\ell = J - 1/2$ amplitude by using Eq. (11). Then the N trajectory, $\alpha_N(\sqrt{s})$, at the resonances will have the form: $\alpha_N(-2.2) = 9/2$, $\alpha_N(-1.68) = 5/2$, $\alpha_N(-0.939) = 1/2$, $\alpha_N(1.675) = 5/2$, $\alpha_N(2.25) = 9/2$ where the masses of the resonances have been expressed in GeV. An updated fit to these resonances has been performed with a trajectory that splits the degeneracy [3]:

$$\alpha_N(\sqrt{s}) = a_0 + a_1\sqrt{s} + a_2s , \quad (12)$$

where a_0 can be eliminated by imposing the condition $\alpha_N(-0.939) = 1/2$. The result of this fit, shown in figure 5, is interesting and such as to justify a deeper analysis.

On the basis of the previous results for the asymptotic behavior of $\mathcal{I}m \alpha(s)$ we perform only one subtraction in Eq. (10) and, for the real part of $\alpha(\sqrt{s})$, we get

$$\begin{aligned} \mathcal{R}e \alpha(\sqrt{s}) = \alpha(0) &+ \frac{\sqrt{s}}{\pi} PV \int_0^\infty \frac{\mathcal{I}m \alpha^+(s')}{\sqrt{s'}(\sqrt{s'} - \sqrt{s})} d\sqrt{s'} \\ &- \frac{\sqrt{s}}{\pi} PV \int_0^\infty \frac{\mathcal{I}m \alpha^-(s')}{\sqrt{s'}(\sqrt{s'} + \sqrt{s})} d\sqrt{s'} , \end{aligned} \quad (13)$$

where only one of the two principal values has to be taken: the first one for $\sqrt{s} > 0$ and the second one for $\sqrt{s} < 0$. It is convenient to consider the equivalent form

$$\begin{aligned} \mathcal{R}e \alpha(\sqrt{s}) = \alpha(0) &+ \frac{\sqrt{s}}{2\pi} PV \int_0^\infty \frac{ds'}{s'(s' - s)} \left(\sqrt{s'} [\mathcal{I}m \alpha^+(s') - \mathcal{I}m \alpha^-(s')] \right. \\ &\left. + \sqrt{s} [\mathcal{I}m \alpha^+(s') + \mathcal{I}m \alpha^-(s')] \right) , \end{aligned} \quad (14)$$

where the simple expression (4), studied before, is re-obtained when $\mathcal{I}m \alpha^+(s) = \mathcal{I}m \alpha^-(s)$. Obviously, the solution of Eqs. (13) and (14) is the same but the proof is not trivial and will be given in Appendix A.

The experimental values of the widths of resonances, symmetric with respect to the axis $\sqrt{s} = 0$ in the $\sqrt{s} - J$ plane, coincide within the errors. Hence their imaginary parts cannot be too different and a minor modification of the previous assumption (3),

$$\mathcal{I}m \alpha^\pm(s) = s^\delta \sum_n c_n \left(\frac{s - s_n}{s} \right)^{\mathcal{R}e \alpha^\pm(s_n)} \cdot \theta(s - s_n) , \quad (15)$$

¹The absence of parity doublets in the low energy part of baryon spectrum as an indication of spontaneous symmetry breaking has been proposed in Ref [10]

seems reasonable in view of the small difference between the trajectories

$$\alpha^\pm(\sqrt{s}) = a_0 \pm a_1\sqrt{s} + a_2s$$

resulting from the fit. The condition $\delta < 1/2$, necessary for the convergence of integrals in Eq. (13), has been implemented in view of the results in the preceding Section. In Eq. (15) $\mathcal{I}m \alpha^\pm(s)$ does not change under the transformation $\sqrt{s} \rightarrow -\sqrt{s}$ and hence, for example, s^δ must be interpreted as $(|\sqrt{s}|^2)^\delta$ while $\sqrt{s_n}$ is always positive.

Let us rewrite Eq. (14) in the form

$$\mathcal{R}e \alpha(\sqrt{s}) = \alpha(0) + \sum_n c_n \mathcal{F}_n(\sqrt{s}) \quad (16)$$

and set $\lambda_n^\pm = \mathcal{R}e \alpha^\pm(s_n)$. With this input in Eq. (14) the expression for $\mathcal{F}_n(\sqrt{s})$ can be easily evaluated. We find

$$\begin{aligned} \mathcal{F}_n(\sqrt{s}) &= \frac{1}{2} \left\{ \left[s^\delta \left(1 - \frac{s_n}{s}\right)^{\lambda_n^+} \tan(\pi\delta) - \frac{\sqrt{s_n} s_n^\delta \Gamma(-1/2 - \delta) \Gamma(1 + \lambda_n^+)}{\sqrt{s} \pi \Gamma(1/2 - \delta + \lambda_n^+)} \right] \times \right. \\ &\quad \times {}_2F_1 \left(1, \frac{1}{2} + \delta - \lambda_n^+; \frac{3}{2} + \delta; \frac{s_n}{s} \right) - \text{the same term with } \lambda_n^+ \rightarrow \lambda_n^- \left. \right] + \\ &\quad + \left[-s^\delta \left(1 - \frac{s_n}{s}\right)^{\lambda_n^+} \cot(\pi\delta) - \frac{s_n^\delta \Gamma(-\delta) \Gamma(1 + \lambda_n^+)}{\pi \Gamma(1 - \delta + \lambda_n^+)} {}_2F_1 \left(1, \delta - \lambda_n^+; 1 + \delta; \frac{s_n}{s} \right) \right. \\ &\quad + \left. \left. \text{the same term with } \lambda_n^+ \rightarrow \lambda_n^- \right] \right\} \theta(s - s_n) \\ &\quad + \frac{1}{2} \left\{ \left[\frac{\sqrt{s} s_n^\delta \Gamma(1/2 - \delta) \Gamma(1 + \lambda_n^+)}{\sqrt{s_n} \pi \Gamma(3/2 - \delta + \lambda_n^+)} \right] \times \right. \\ &\quad \times {}_2F_1 \left(1, \frac{1}{2} - \delta; \frac{3}{2} - \delta + \lambda_n^+; \frac{s}{s_n} \right) - \text{the same term with } \lambda_n^+ \rightarrow \lambda_n^- \left. \right] + \\ &\quad + \left[\frac{s s_n^\delta \Gamma(1 - \delta) \Gamma(1 + \lambda_n^+)}{s_n \pi \Gamma(2 - \delta + \lambda_n^+)} {}_2F_1 \left(1, 1 - \delta; 2 - \delta + \lambda_n^+; \frac{s}{s_n} \right) \right. \\ &\quad + \left. \left. \text{the same term with } \lambda_n^+ \rightarrow \lambda_n^- \right] \right\} \theta(s_n - s) . \quad (17) \end{aligned}$$

The widths can be found by first calculating the derivative of $\alpha'_R(\sqrt{s})$. The result can be written as

$$\alpha'_R(\sqrt{s}) \equiv \frac{d\mathcal{R}e\alpha(\sqrt{s})}{d\sqrt{s}} = \sum_n c_n \mathcal{D}_n(\sqrt{s}) .$$

By comparison with a Breit-Wigner resonance of mass M , where M can be positive or negative in this context, we get the total width

$$\Gamma = \frac{2\mathcal{I}m \alpha(M^2)}{|\alpha'_R(M)|} . \quad (18)$$

The calculation of $\alpha'_R(\sqrt{s})$ parallels the one already done in the preceding Section and the explicit form of $\mathcal{D}_n(\sqrt{s})$ will be shown in Appendix B.

5 Application to the nucleon trajectory

In this section we apply the formalism to the nucleon trajectory.

First we fit the real part of the amplitude using the following form of the trajectory:

$$\alpha^\pm(\sqrt{s}) = a_0 \pm a_1\sqrt{s} + a_2s , \quad (19)$$

where the sign “+” corresponds to the N^+ trajectory which contains the baryons $N(939) \frac{1}{2}^+$, $N(1680) \frac{5}{2}^+$, $N(2220) \frac{9}{2}^+$ and $N(2700) \frac{13}{2}^+$ [7], while the sign “-” corresponds to the N^- trajectory, which contains $N(1675) \frac{5}{2}^-$ and $N(2250) \frac{9}{2}^-$ [7].

Thus, we obtain $\alpha(0) = -0.398$, $a_1 = -(0.86 \pm 1.36) \cdot 10^{-2} \text{ (GeV}^{-1}\text{)}$ and $a_2 = 1.03 \pm 0.01 \text{ (GeV}^{-2}\text{)}$ ($\chi^2/\text{d.o.f} = 0.57$). The parameter a_0 is eliminated from the fit by using the condition:

$$\alpha^+(m_n) \equiv a_0 - a_1 m_n + a_2 m_n^2 = 1/2 , \quad (20)$$

where m_n is the nucleon mass.

Using these values of the parameters we calculate $\mathcal{R}e \alpha^\pm(s_n)$, where $n = 1, 2, x$ and $s_1 = (m_\pi + m_N)^2 = 1.16 \text{ GeV}^2$, $s_2 = 2.44 \text{ GeV}^2$ and $s_x = 11.7 \text{ GeV}^2$. In what follows, s_2 will be used as a parameter. The final result does not depend very significantly on s_x , so its value is fixed at 11.7 GeV^2 .

Then we set $\lambda_n^\pm = \mathcal{R}e \alpha^\pm(s_n)$ and continue the recursive fitting procedure using formulas (14) and (18). After 10 steps the procedure converges and the result we arrive at for the values of the parameters is $c_1 = 0.22 \pm 0.02$, $c_2 = 0.37 \pm 0.09$, and $c_x = 18.4 \pm 1.1$, $s_2 = 2.4 \pm 0.2 \text{ GeV}^2$, $\delta = 0.49 \pm 0.09$, ($\chi^2/\text{d.o.f} = 1.0$). The intercept of the trajectory does not change visibly, $\alpha(0) = -0.42$.

The results are presented in figures 5 and 6.

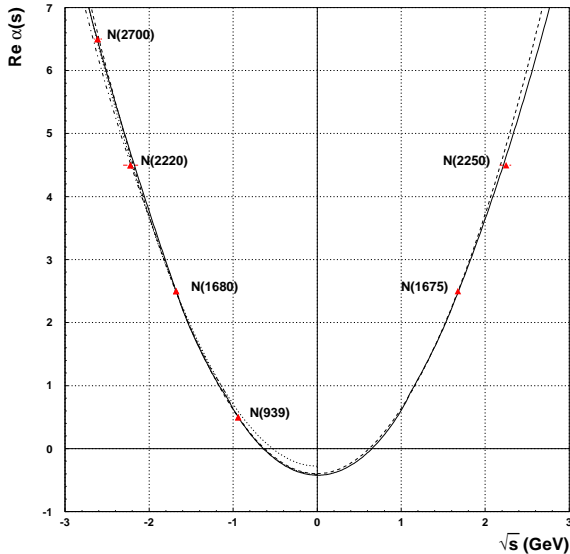


Figure 5: The real part of N trajectory. The dashed line corresponds to the result of the fit with Eq. (19), the solid line corresponds to the final result. The dotted line corresponds to the linear fit.

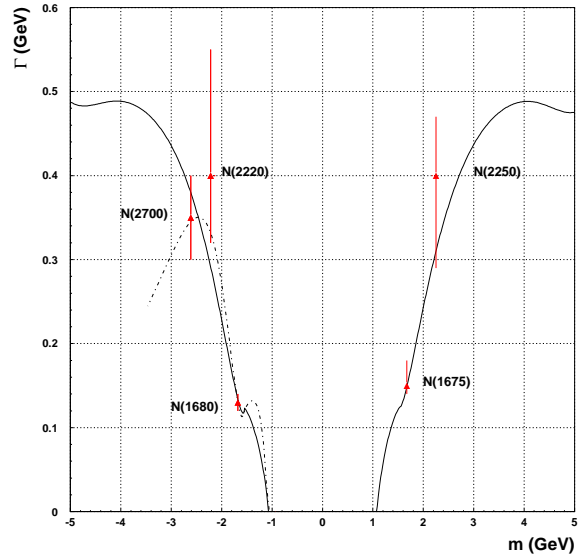


Figure 6: The width of N trajectory. The dotted-dashed line corresponds to the fit with the simplified model, the solid line corresponds to the final result.

6 Concluding remarks

The main problem in constructing models for Regge trajectories resides in the difficulty of making the nearly linear rise of the real part in the whole range of observed resonances compatible with the presence of a sizable imaginary part. Figures (1) and (3) suggest that this difficulty has been overcome. The complexity of the problem reveals itself in the imaginary part of the trajectories as shown in figures (2) and (4).

The main assumptions regard only the imaginary part of the trajectory. This, through dispersion relations, determines completely the analytic structure of the model. The real part, the slope and the widths of the resonances follow from the hypothesis that the contributions of different thresholds are additive. There is no first-principle reason for this constraint, it is imposed only for simplicity sake.

In the simple model of Section 2 we found a physical interpretation for the position of the thresholds that the N trajectory inherits from the partial wave amplitude for the pion-nucleon scattering. However, such interpretation becomes problematic when the MacDowell symmetry is implemented. In this case, we must consider the thresholds, above the first one, as effective thresholds. This is always true for the last threshold s_x whose position is only weakly constrained from the experimental data. s_x can move to higher values of s if it is required from the discovery of new baryonic resonances.

Data for the excited states of the baryons are often insufficient for a fit of the parameters appearing in the (oversimplified) imaginary part of the trajectory. For this reason our analysis cannot be extended to strange and charmed baryons. Furthermore, for the nucleon, our findings do not put strong constraints on a future search of new nucleonic states. Approximate symmetries or dynamical models, not accounted for in this paper, could help in obtaining more precise predictions when complemented by analyticity and unitarity. A “global” fit to baryonic trajectories could be an important step forward a deeper understanding of their structure. This possibility will be explored elsewhere.

Appendix A

In this Appendix we collect the formulas that show how Eq. (13) can be solved and the equivalence of the solution with the one of Eq. (14). Inserting Eq. (15) in Eq. (13) one obtains

$$\begin{aligned} \mathcal{A}_n(\sqrt{s}) &= PV \int_0^\infty s'^{\delta-1/2-\lambda_n^+} (s' - s_n)^{\lambda_n^+} \frac{1}{\sqrt{s'} - \sqrt{s}} d\sqrt{s'} \theta(s' - s_n) - \\ &- \int_0^\infty s'^{\delta-1/2-\lambda_n^-} (s' - s_n)^{\lambda_n^-} \frac{1}{\sqrt{s'} + \sqrt{s}} d\sqrt{s'} \theta(s' - s_n). \end{aligned} \quad (\text{A-1})$$

Consider now the second integral on the right hand side of Eq. (A-1). Substituting $u = \sqrt{s_n/s'}$ we get

$$\int_{\sqrt{s_n}}^\infty s'^{\delta-1/2-\lambda_n^-} (s' - s_n)^{\lambda_n^-} \frac{1}{\sqrt{s'} + \sqrt{s}} d\sqrt{s'} = (\sqrt{s_n})^{2\delta-1} \int_0^1 \frac{u^{-2\delta}(1-u^2)^{\lambda_n^-}}{1 + \sqrt{s/s_n} u} du. \quad (\text{A-2})$$

We obtain

$$\begin{aligned}
& \int_0^1 \frac{u^{-2\delta}(1-u^2)^{\lambda_n^-}}{1+\sqrt{s/s_n}u} du = \\
& \frac{1}{2}\Gamma(1+\lambda_n^-) \left[-\sqrt{\frac{s}{s_n}} \frac{\Gamma(1-\delta)}{\Gamma(2+\lambda_n^- - \delta)} {}_2F_1 \left(1, 1-\delta; 2-\delta+\lambda_n^-; \frac{s}{s_n} \right) + \right. \\
& \left. + \frac{\Gamma(1/2-\delta)}{\Gamma(3/2+\lambda_n^- - \delta)} {}_2F_1 \left(1, 1/2-\delta; 3/2-\delta+\lambda_n^-; \frac{s}{s_n} \right) \right], \tag{A-3}
\end{aligned}$$

that is a convenient expression when $s_n > s$. However, when $s > s_n$, it is necessary to perform an analytic continuation that, in the general case considered here ², gives

$$\begin{aligned}
& \int_0^1 \frac{u^{-2\delta}(1-u^2)^{\lambda_n^-}}{1+\sqrt{s/s_n}u} du = \\
& \frac{1}{2} \left[\frac{\Gamma[\lambda_n^- + 1]\Gamma(-\delta)}{\Gamma(1+\lambda_n^- - \delta)} \sqrt{\frac{s_n}{s}} {}_2F_1 \left(1, \delta - \lambda_n^-; 1 + \delta; \frac{s_n}{s} \right) - \right. \\
& \left. \frac{\Gamma(1+\lambda_n^-)\Gamma(-1/2-\delta)}{\Gamma(1/2+\lambda_n^- - \delta)} \frac{s_n}{s} {}_2F_1 \left(1, 1/2 + \delta - \lambda_n^-; 3/2 + \delta; \frac{s_n}{s} \right) + \right. \\
& \left. + \pi \left(\frac{s_n}{s} \right)^{1/2-\delta} \left(1 - \frac{s_n}{s} \right)^{\lambda_n^-} \frac{1}{\sin(\pi\delta) \cos(\pi\delta)} \right]. \tag{A-4}
\end{aligned}$$

Eqs. (A-3) and (A-4) give the result for the integral in Eq. (13) in all possible cases.

Of the first integral in Eq. (A-1) we must take the principal value. By multiplying the numerator and denominator of the integrand by $(\sqrt{s'} + \sqrt{s})$ we get

$$\begin{aligned}
& PV \int_0^\infty s'^{\delta-1/2-\lambda_n^+} (s' - s_n)^{\lambda_n^+} \frac{1}{\sqrt{s'} - \sqrt{s}} d\sqrt{s'} \theta(s' - s_n) = \\
& = \frac{\sqrt{s}}{2} PV \int_0^\infty \frac{y^{\lambda_n^+} (y + s_n)^{\delta-1-\lambda_n^+}}{y - (s - s_n)} dy + \frac{1}{2} PV \int_0^\infty \frac{y^{\lambda_n^+} (y + s_n)^{\delta-1/2-\lambda_n^+}}{y - (s - s_n)} dy, \tag{A-5}
\end{aligned}$$

that can be easily solved since both integrals, in the second row of Eq. (A-5), are of the same form of the integrals solved before. Since $\mathcal{R}e\alpha(\sqrt{s})$ is an analytic function of \sqrt{s} Eqs (A-3) and (A-4) hold also when $\sqrt{s} < 0$.

Appendix B

It is easy to show that the derivative of $\mathcal{R}e\alpha(\sqrt{s})$ gives for $\mathcal{D}_n(\sqrt{s})$ the following cumbersome expression:

$$\begin{aligned}
\mathcal{D}_n(\sqrt{s}) &= \frac{1}{2} \left\{ \left[2s^{\delta-3/2} \left(1 - \frac{s_n}{s} \right)^{\lambda_n^+ - 1} (\lambda_n^+ s_n + \delta(s - s_n)) \tan(\pi\delta) \right. \right. \\
& \left. \left. + \frac{s_n^{\delta+1/2}}{s} \frac{\Gamma(-1/2-\delta)\Gamma(1+\lambda_n^+)}{\pi\Gamma(1/2-\delta+\lambda_n^+)} \left({}_2F_1 \left(1, \frac{1}{2} + \delta - \lambda_n^+; \frac{3}{2} + \delta; \frac{s_n}{s} \right) \right) \right] \right\}
\end{aligned}$$

²In the general case $1-c$, $b-a$ and $c-b-a$ in $F(a, b; c; z)$ are not integers.

$$\begin{aligned}
& + \frac{2(\delta - \lambda_n^+ + 1/2)}{\delta + 3/2} \frac{s_n}{s} {}_2F_1 \left(2, \frac{3}{2} + \delta - \lambda_n^+; \frac{5}{2} + \delta; \frac{s_n}{s} \right) \\
& - \text{the same term with } \lambda_n^+ \rightarrow \lambda_n^- \Big] + \\
& + \left[-2s^{\delta-3/2} \left(1 - \frac{s_n}{s} \right)^{\lambda_n^+-1} (\lambda_n^+ s_n + \delta(s - s_n)) \cot(\pi\delta) \right. \\
& + 2 \frac{s_n^{\delta+1} (\delta - \lambda_n^+) \Gamma(-\delta) \Gamma(1 + \lambda_n^+)}{\pi s^{3/2} (1 + \delta) \Gamma(1 - \delta + \lambda_n^+)} {}_2F_1 \left(2, 1 + \delta - \lambda_n^+; 2 + \delta; \frac{s_n}{s} \right) \\
& + \left. \text{the same term with } \lambda_n^+ \rightarrow \lambda_n^- \right] \Big\} \theta(s - s_n) \\
& + \frac{1}{2} \left\{ \left[s_n^{\delta-3/2} \frac{\Gamma(1/2 - \delta) \Gamma(1 + \lambda_n^+)}{\pi \Gamma(3/2 - \delta + \lambda_n^+)} \left(s_n {}_2F_1 \left(1, \frac{1}{2} - \delta; \frac{3}{2} - \delta + \lambda_n^+; \frac{s_n}{s} \right) \right. \right. \right. \\
& + \left. \left. \frac{(1 - 2\delta)s}{\lambda_n^+ - \delta + 3/2} {}_2F_1 \left(2, \frac{3}{2} - \delta; \frac{5}{2} - \delta + \lambda_n^+; \frac{s_n}{s} \right) \right) \right. \\
& - \left. \left. \text{the same term with } \lambda_n^+ \rightarrow \lambda_n^- \right] + \right. \\
& + \left. \left[2 \frac{s_n^{\delta-1} \Gamma(1 - \delta) \Gamma(1 + \lambda_n^+)}{\pi \Gamma(2 - \delta + \lambda_n^+)} \sqrt{s} {}_2F_1 \left(1, 1 - \delta; 2 - \delta + \lambda_n^+; \frac{s_n}{s} \right) \right. \right. \\
& + \left. \left. \text{the same term with } \lambda_n^+ \rightarrow \lambda_n^- \right] \right\} \theta(s_n - s) . \tag{B-1}
\end{aligned}$$

References

- [1] A.E. Inopin, hep-ph/0110160.
- [2] V. Barger and D. Cline, Phys. Rev. **155** (1967) 1792; V. Barger, E. Michael and R.J.N. Phillips, Phys. Rev. **185** (1969) 1852.
- [3] C.B. Chiu and J.D. Stack, Phys. Rev. **153** (1967) 1575.
- [4] N.I. Glushko, N.A. Kobylinsky and V.V. Timokhin, ITP-82-10 E.
- [5] A.B. Kaidalov and A.F. Nilov, Sov. J. Nucl. Phys. **41** (1985) 490 [Yad. Fiz. **41** (1985) 768].
- [6] A. Tang and J.W. Norbury, Phys. Rev. **D62** (2000) 016006.
- [7] The data on baryon masses and widths can be found in: K. Hagiwara et al., Phys. Rev. D **66**, (2002) 010001.
- [8] V.N. Gribov, Sov. Phys. JETP **16** (1963) 1080 [J. Exptl. Theor. Phys. **43** (1962) 1529].
- [9] S.W. MacDowell, Phys. Rev. **116** (1959) 774.
- [10] L. Ya Glizman, hep-ph/0105222; hep-ph/0309334.

- [11] P.D.B. Collins, *Introduction to Regge Theory and High Energy Physics*, Cambridge University Press (1977)
- [12] A. Degasperis and E. Predazzi, *Nuovo Cimento* **65A** (1970) 764.
- [13] S. Filipponi, G. Pancheri and Y. Srivastava, *Phys. Rev D* **59** (1999) 076003.
- [14] R. Fiore et al., *Particles and Nuclei* **31** (2000) 46; *Nucl. Phys. B (Proc. Suppl.)* **99** (2001) 68.
- [15] R. Fiore et al., *Eur. Phys. J. A* **10** (2001) 217.
- [16] A.O. Barut and D.E. Zwanziger, *Phys Rev.* **127** (1962) 974;
V.N. Gribov and Ya.I. Pomeranchuk, *Nucl. Phys.* **38** (1962) 516;
R. Oehme, in *Scottish Summer School 1963*, edited by R.G. Moorhouse et al., Edinburgh (1964) p. 129;
N.A. Kobilinsky and A.B. Prognimac, *Acta Phys. Polonica* **B9** (1978) 149 and earlier references therein.
- [17] J.A. Sakmar, *Phys. Rev. B* **135** (1964) 249;
B. Desai, *Phys. Rev. Lett.* **17** (1966) 498.
- [18] A. Erdélyi et al., *Tables of Integral Transforms*, Vol II (McGraw-Hill, New York, 1953)